RESEARCH PAPER

Shear Performance of Steel Fiber Reinforced Concrete Beams Without Stirrups: Experimental Investigation

T. T. Bui[1] · W. S. A. Nana[2] · B. Doucet-Ferru[2] · A. Bennani[3] · H. Lequay[4] · A. Limam[5]

Abstract

Over the past century, a considerable amount of research has been conducted to study the brittle behavior of traditional concrete. Currently, fiber reinforcement material appears as an effective way to enhance general concrete performance under diverse loads. In the present study, an experimental investigation of the steel fibers' effect on the bending behavior of concrete beams is performed. The main objectives were first to see whether the use of steel fibers allows the total substitution of traditional transverse reinforcement (stirrups) and second to examine the effect of a combination of steel fibers and longitudinal rebars. The experimental program includes four beam specimens of dimensions 1700 mm × 80 mm × 150 mm. The results show that the fiber volume fraction of 100 kg/m^3 of uncoated steel fibers, which corresponds to 1.27% fiber volume fraction, can be used to replace the transverse reinforcement. Besides, the obtained results show that the combination of the steel fibers with longitudinal reinforcement is necessary to obtain a better resistance under bending.

Keywords Reinforced concrete beams · Steel fibers · High-strength concrete · Bending behavior

✉ T. T. Bui
tan-trung.bui@insa-lyon.fr

W. S. A. Nana
wendpanga-serge-auguste.nana@insa-lyon.fr

B. Doucet-Ferru
baptiste.doucet-ferru@insa-lyon.fr

A. Bennani
abdelkrim.bennani@hesge.ch

H. Lequay
herve.lequay@lyon.archi.fr

A. Limam
ali.limam@insa-lyon.fr

1   GEOMAS, INSA Lyon, University of Lyon, Lyon, France

2   INSA Lyon, Lyon, France

3   HEPIA, Geneva, HES-SO University of Applied Sciences Western Switzerland, Geneva, Switzerland

4   ENSAL, MAP-ARIA, UMR 3495, Vaulx-en-Velin, France

5   IFSTTAR, GERS, RRO, Bron, France

1 Introduction

Over the past century, a considerable amount of research has been conducted to study the brittle behavior of traditional concrete. Indeed, plain unreinforced cement-based materials largely used for construction such as concrete are brittle and are prone to cracking when subjected to relatively small tensile stresses. This deficiency has been solved with the use of continuous steel reinforcing bars that are strategically placed to withstand tensile stresses in the structural element. However, although steel reinforcement can improve the flexural capacity of the plain concrete, the concrete crack occurs almost inevitably even under service loads [1]. It is therefore essential to improve the concrete tensile performance and to guarantee the reinforced concrete (RC) structures serviceability, durability and safety. Currently, fiber reinforcement material appears as an effective way to enhance general concrete performance under diverse loads. Test results as conducted in [2] show that the concrete flexural capacity increases with the increase in the steel fiber volume fraction varying from 0.25 to 0.50%. Several other researchers also reached the same conclusion with hybrid fiber and macro-polypropylene fiber type [3, 4]. Steel fiber effects on the shear

resistance of beams with and without stirrups have also been investigated [5–7]. The authors showed that the nominal stress at shear cracking and the ultimate shear strength increased with increasing the fiber's volume. Concerning the fire resistance of concrete structures, the experimental study conducted in [8] shows that a mix of polypropylene fibers (0.75 kg/m^3) and steel fibers (60 kg/m^3) permits to avoid spalling preventing any macroscopic damage. Using several and distinct materials conducts to the question of multi-material topology optimization as studied in [9, 10]. The experimental programs of [11, 12] demonstrated the beneficial effect of adding fibers against dynamic loads including cyclic and impact load conditions. It has been highlighted that a good long straight steel fiber orientation is effective in improving the impact resistance of ordinary concrete.

The concrete fiber material proved its reliability in some structural and non-structural applications. Examples of practical applications of steel fiber-reinforced concrete (SFRC) include ground- and pile-supported slabs, tunnel linings, various precast elements, raft foundations, industrial pavement, complex architectural forms as Marseille museum MuCEM and others [13]. For some structural applications, steel fibers provide the only reinforcement as for slabs on piles, foundation slabs, deck floor, suspended elevated slabs, while in other cases they are combined with traditional steel bars and used in a supplementary role, either for a better cracking inhibition or to improve resistance to material deterioration. The main distinctive feature of SFRC, in contrast to conventional reinforced concrete, concerns improvements in the energy absorption properties of the material and the ability of the material to carry tensile stresses after crack initiation. The SFRC can locally reinforce the cracked matrix by transferring stresses across the fractured surface and consequently lower the cracking propagation and cracks opening. While conventional concrete accomplishes a limited stress transfer across cracks by an aggregate interlocking phenomenon, fibers' presence enables the significant transfer of tensile loads across cracks until the fiber either pulls out or fails. In addition, SFRC can be profitable over traditional reinforcement as a result of shorter construction time and ease of placement. Indeed, the development of newer precast structural elements includes the request for lightweight, implementation versatility, reduced construction time and cost and higher durability performance. All of these requirements interact and affect each other and need to be addressed during the design process. In this context, the properties of SFRC in prefabricated structural elements allow a more efficient construction process.

Nowadays, fibers are produced from different materials such as steel (SFRC), glass, carbon and synthetic material such as polypropylene fiber-reinforced concrete (PP-FRC) or polyvinyl alcohol (PVA) fiber-reinforced concrete. Each type of fiber has its specific benefits. However, steel fiber is the most common one. Performances of SFRC depend on many factors. As mentioned above, two failure scenarios are possible: either the failure of fibers or the pull-out of fibers from the cement concrete matrix. The second scenario is preferable because it is more ductile and acts as an energy absorber. In other words, for the fiber to be pulled out, it should tense significantly and yield. Consequently, this process will absorb a great amount of energy. One of the factors that affect the failure type is the bond between steel fiber and concrete. The other factors affecting the SFRC include the fiber material properties (fiber strength, stiffness, Poisson's ratio and fiber ductility), the fiber type and geometry (smooth, end-hooked, crimped and twisted fibers, aspect ratio), fiber dosage and concrete matrix properties (matrix strength, stiffness, Poisson's ratio). The transfer of stress across cracks influences the crack opening process and may result in various load deformation responses under direct tensile or flexural loading that include softening and hardening post-cracking responses. The softening or hardening nature of the post-cracking law is dependent on all the fiber's properties mentioned above. For softening, the ultimate load-carrying capacity corresponds to the first crack strength and is typically accompanied by a concentration of deformation, or localization, in a single crack. If a higher load-carrying capacity occurs after the first crack strength, the composite is considered to be hardening, which is typically accompanied by the formation of multiple cracks with controlled width. Overall, low-fiber-volume contents will exhibit softening behavior, while high-volume will show a hardening response. However, hardening behavior could also be achieved by adding a relatively small volume < 2% of randomly distributed fibers as found in some studies [14].

Strain hardening is usually observed when fibers are added in the matrix of high-strength or ultra-high-strength concrete and has been proven by researchers [15, 16]. These materials are of great interest for applications related to large energy absorption and crack width control. In other words, all the benefits related to the use of high-performance fiber-reinforced concrete have made it ideal for the modular concrete structures or constructions [17].

2 Research Aims

The present study focuses on the implication of steel fibers on the bending and shear behavior of high-strength concrete beams used for modular construction. The contribution provided by the fibers is compared to the case of conventional steel bar-reinforced concrete. The main objectives are first to see whether the use of a high volume

of steel fibers allows the total or partial substitution of the stirrups, which corresponds to the traditional transverse reinforcement, and second to examine the effect of a combination of fibers and longitudinal reinforcement. It is to highlight that the modular home slabs and walls comprise peripherally ribs that serve as stiffeners. These ribs are armed with two Φ10 steels bars, which participate with the fibers in the flexural strength. For steel fibers' effect on the bending behavior of RC beams, the literature review reveals studies with various types of fibers having different properties, different concrete strength and formulations and study configurations, and sometimes, the results cannot be directly extrapolated [18]. Some laboratory tests of literature are not always representative of real conceptions. Fiber reinforcement has been in use over the last 30 years, but no unified guideline for the design exists. Moreover, most of the studies are performed with a minimum longitudinal reinforcement ratio, and currently in engineering design offices, structural beams made of SFRC are also reinforced with longitudinal steel bars for shear ligatures. A beam reinforced only with fiber is extremely rare. Most SFRC has softening behavior and reserved in practice only for non-structural applications. In this study, we evaluate the possibility of manufacturing only fiber-reinforced concrete beams with improved tensile material properties related to its hardening instead of softening behavior. This will enhance the safety with a conservative design. For this purpose, high fiber quantity was used, above 1%, the limit generally underlined to cause problems of concrete workability. Thanks to the specific formulation here adopted, one innovative approach used in our study lies in the combined use of a high volume of fibers ($V_f > 1\%$) and a flowable self-placing concrete to improve workability.

The experimental program included four beam specimens. The first beam is a 2Φ10 bottom longitudinal steel bar-reinforced beam without shear reinforcement. The second beam is similar to the first but with shear reinforcement. The third specimen is an entirely SFRC beam with a volume fraction of 1.27% (100 kg/m^3) and without rebars. The last beam is similar to the third with similar longitudinal reinforcement arrangement as for the first and second beams. The specimens were chosen to represent modular house construction, resulting in more moderate sections relative to the building. These structures must be lightweighted, because the elements must be transported. Furthermore, the reinforcement considered in the tensioned part of the beam (2HA10) allows to guaranty shear failure in the case of the lack of stirrups. However, the stirrups permit to block this type of failure and thus to return to a bending rupture. Switching from one configuration to another therefore makes it possible to study the contribution of the fibers in each case. The fibers rate is chosen very high (100 kg/m^3). It is rare to have more than 80 kg/m^3 of

fibers because the fluidity of the concrete is then questioned, and moreover, it is very difficult to have a uniform distribution of fibers. In our case, a specific formulation with the use of an additive allowed to overcome these problems.

3 Experimental Program

3.1 Tests for Material Properties of Ordinary Concrete and SFRC

Before the beam tests, material characterization of the concrete and the SFRC was carried out. Uniaxial compressive tests, tensile tests (splitting) and flexural prismatic beam tests under four-point loading were performed to assess the material properties. Note that several methods are proposed in the literature to study the tensile behavior of SFRC. There is a general need in structural engineering for standard methods to quickly, easily and reliably verify that the material properties achieved in situ comply with the parameters assumed in the design. When using a direct uniaxial tensile test on notched specimens [19] and unnotched specimens [20], the stress-crack opening or stress–strain properties of SFRC can be derived directly. However, the direct tension test method samples are laborious and difficult to implement field quality control purposes. Several standard flexural test methods exist, based on beams and plates geometries, to indirectly assess the tensile properties of SFRC. Most design codes and recommendations proposed the use of notched three-point bending tests: fib Model code [21], Swedish standard [22], European test recommendation [23, 24], Japan Concrete Institute [25]. Such tests provide an estimate of tensile properties based on simplified assumption and analysis of the obtained load–deformation (strain), load–deflection, or load–CMOD curves. In most cases, simplified strain compatibility and stress block analysis of a layered cross section (i.e., an assumed stress profile) are required to compute the design ultimate moment capacity of a structural element [26]. Therefore, two simplified assumptions are made, one for deriving the tensile properties from the flexural test and a second in the design model for calculating the plastic moment capacity.

In our study, the tensile performance of the SFRC was evaluated by performing flexural un-notched prismatic beam tests under four-point loading according to the French Association of Normalization [27]. Five beam specimens, 70 mm high, 70 mm wide, and 280 mm long, were manufactured and tested on the same day as beam strength tests. The span of the beam between the supports was 252 mm. Two loading points, 84 mm apart, were applied to the top surface of the beam at the mid-span. The

test was displacement-controlled with a loading rate set to 1 mm/min. The vertical displacement was measured using a linear variable differential transformer (LVDT) located at the backside of the beam at the mid-span. The test configuration is illustrated in Fig. 1. In addition, to evaluate the compressive strengths and tensile strengths by splitting test of the SFRC, six cylinder specimens (diameter 110 mm and height 220 mm) were prepared and tested. The cylinders and prismatic beams were cured in the same conditions as the beams in a room have a temperature of 20 °C. The goal was to keep the concrete in an environment close to that of the real structure. Afterward, the casting surface of cylinders in contact with the loading platens was made flat by the supply of sulfur in order to ensure uniform contact and thus avoid as much as possible, any load eccentricities which would lead to parasitic moments. A monotonical load was applied for specimens using a Perrier hydraulic press with a capacity of 1000 kN. Furthermore, the mechanical properties of the ordinary concrete were also evaluated and compared to that of the

SFRC in order to examine the effects of the inclusion of steel fiber on concrete mechanical performance. For this purpose, six cylinder specimens and three prismatic beams were fabricated for compressive, splitting and flexural tensile tests, respectively. The modulus of elasticity was also experimentally obtained.

In our study, 100 kg/m^3 of uncoated steel fibers was used, which corresponds to 1.27% fiber volume fraction. The hooked-end fibers (Dramix RC-65/35-BN brand) were made from cold-drawn steel wire, deformed with hooked ends, glued in bundles. The fibers had a length of 35 mm and a diameter of 0.55 mm, leading to an aspect ratio (l/d) of 64. Figure 2 depicts the typical fiber dimensions. The tensile strength of the fiber was approximately 1100 MPa. Note that a possible inconvenience associated with SFRC is that the addition of fibers to traditional concrete can cause problems in workability when high fiber quantities are used (1% and above) and in situations where high ratios of steel reinforcement are used. One innovative approach used in our study lies in the combined use of SFRC and a
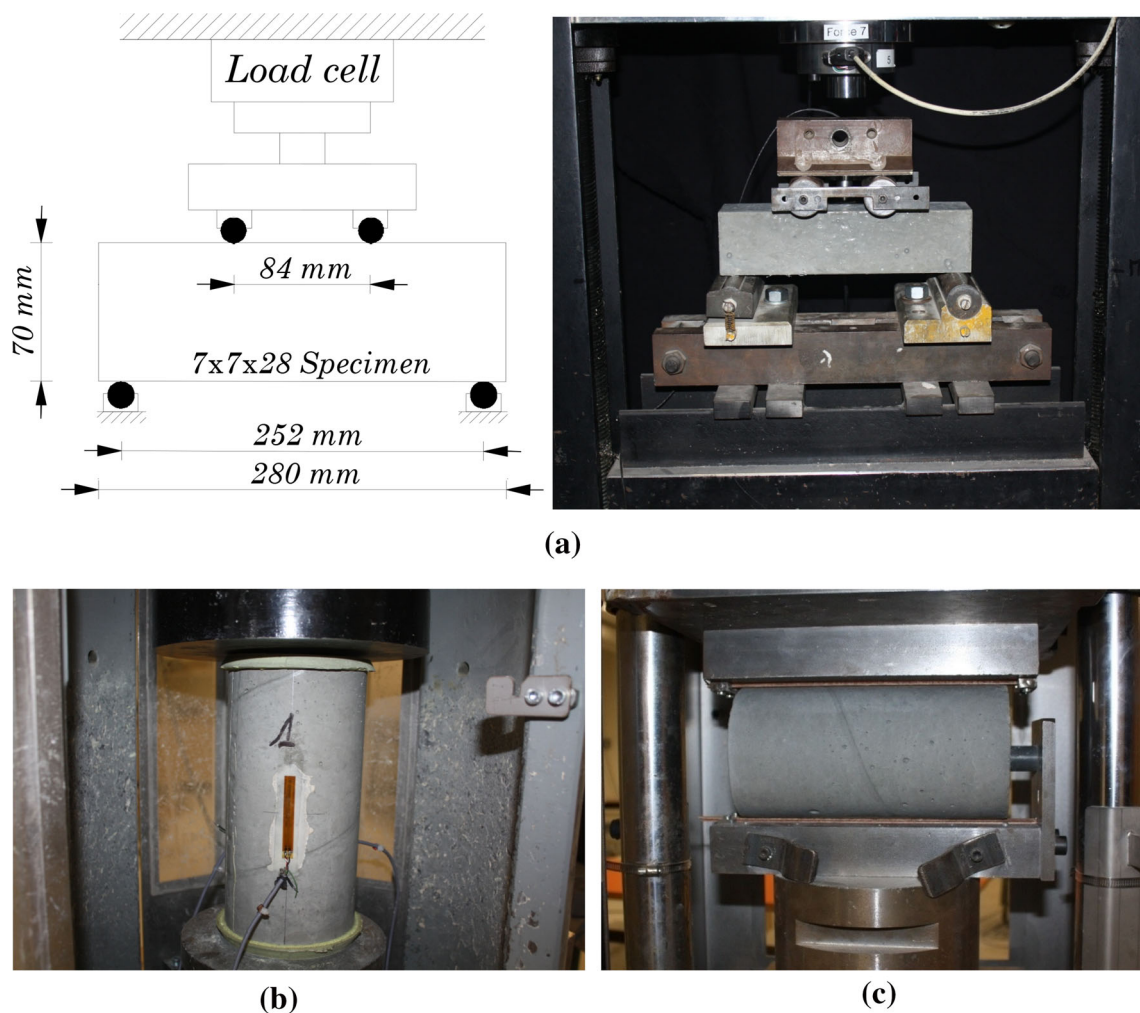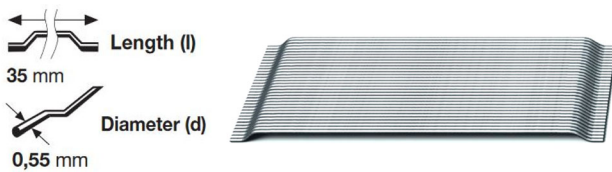

Fig. 1 a Four-point bending test setup, b uniaxial compression test setup, c splitting test setup

Fig. 2 Geometrical properties of Dramix RC-65/35-BN hooked-end steel fibers

flowable self-consolidating concrete to improve workability and facilitate placement. Table 1 summarizes the mixture proportions of SFRC and ordinary concrete. CEM I 52.5 Portland cement was used. The ratio of water to cement (W/C) was 0.38, and the unit weights of cement and water were 760 and 290 kg/m^3, respectively. Ecocem Ground granulated blast furnace slag of 225 kg/m^3 was added to give concrete an excellent durability and long-term strength. Fine crushed and rolled sand, and gravel with a maximum grain size of about 6 mm were used for fine and coarse aggregates, respectively. The ratio of sand-to-total aggregate (s/a) was 0.49. In order to improve the workability of SFRC mixtures, a superplasticizing additive for concrete Dynamon NRG 1040 was used with an amount of 13.5 kg/m^3. A quantity of 0.2–2% of the weight of cement for traditional concrete and 0.2–2% of the weight of fine elements for self-compacting concrete is recommended. A viscosity agent (0.25 kg/m^3) was added to limit the aggregates and fibers segregation and thus prevent them from falling at the bottom of the molds.

3.2 Test Specimens and Setup

An experimental program was conducted in order to investigate the steel fibers' effect on the behavior of RC beams when submitted to four-point bending. The main objective was firstly to see whether the use of steel fibers allows the total or partial substitution of traditional transverse reinforcement and secondly to examine the effect of a combination of fibers and longitudinal reinforcement. To this end, four beams were produced for testing. For easy reference, each fiber-reinforced beam was labeled with a "BF" and traditionally reinforced beams without fibers labeled with a "B." The geometrical properties and reinforcement details of all the beams are illustrated in Fig. 4. All of the beams had nominally identical cross-sectional

dimensions of 80×150 mm^2, effective depths of 125 mm for those with longitudinal reinforcement, and a total length of 1700 mm corresponding to a clear span length of 1500 mm. The distance between the two loading points in the flexural area was 500 mm. The shear span a was 500 mm, so a value of 4.0 was obtained for the ratio of a/d. As it can be seen in Fig. 4, the first beam B1 is a steel bar-reinforced beam without shear reinforcement. The longitudinal reinforcement consisted of four steel bars: two bars with a diameter of 6 mm in the top layer and two others with a diameter of 10 mm in the bottom layer. The bars in the bottom layer correspond to a reinforcement ratio of $\rho = 1.30\%$ and represent approximately six times the minimum reinforcement ratio ρ_{min} calculated according to European code [28] for a C80 concrete class. The second beam B2 is similar to the first one with additional shear reinforcement. The shear reinforcement consisted of vertical stirrups with a diameter of 6 mm, spaced 100 mm apart in the probable shear zone and 150 mm in the flexural zone. The third specimen BF1 is an entirely SFRC with a fiber volume fraction of 1.27% (100 kg/m^3). The last beam BF2 is similar to BF1 with additional identical top and bottom longitudinal reinforcement as in B1 and B2. The average Young modulus, yield strength and specific yielding deformation of the longitudinal bars were 200 GPa, 500 MPa and 0.25%, respectively.

It must first be underlined that in this study, the shear reinforcement consisting of vertical stirrups with diameter of 6.0 mm, spaced 10 cm apart, leads to a reinforcement ratio $\rho w = 1.26\%$, which represents approximately 8 times the minimum shear reinforcement ratio ($\rho w_{min} = 0.15\%$) required according to Eurocode 2.

Referring to literature, some studies have also examined the possibility of using steel fibers as shear reinforcement in concrete elements. The research [29] on beams showed that the use of hooked steel fibers in a volume fraction greater than or equal to 0.75% could be used in place of the minimum stirrup reinforcement required. In [30], an experimental study on SFRC beams, the obtained results showed that a relatively low amount of fibers less than 1.0% could significantly improve the shear strength of concrete beams. In [5] study, for concrete beams without stirrups and with shear span-depth ratio a/d equal to 2, where shear load is promoted compared to bending load, it

Table 1 Mixture proportions

Cement CEM I 52.2 (kg/m^3)	Ground granulated blast furnace slag (kg/m^3)	Crushed sand 0/4 mm (kg/m^3)	Rolled sand 0/4 mm (kg/m^3)	Gravel 0/6 mm (kg/m^3)	Water (kg/m^3)	Superplasticizing additive (kg/m^3)	Viscosity agent (kg/m^3)	Fibers (kg/m^3)
760	225	290	290	590	290	13.5	0.25	100

has been noted that as the steel fiber volume increased to 0.5 and 0.75%, respectively, the failure mode changed to a combination of shear and flexure, with significant diagonal shear cracks and vertical flexural cracks both formed.

At last, it is important to note that more experimental research has to be carried out to get more information about optimizing shear behavior when replacing different shear stirrups' configuration by steel fibers.

Figure 3 shows the test setup where the simply supported reinforced concrete beams are subjected to quasi-static loading using a hydraulic jack. The load, measured with a load cell, is applied with a slow speed of 0.60 kN/min and distributed in two loading application points. In order to investigate the strain behavior of the two bottom longitudinal rebars of the beam, two electric resistance strain gauges were bonded at their central section. Three strain gauges, bonded to the concrete, measured longitudinal strains at the compression zone of the beams. To measure the beam deflection, two linear variable differential transformers LVDT1 and LVDT2 were installed underneath the center of the beam and on the loading point, respectively. Gauges and LVDT positions are illustrated in Fig. 4. The measurements were recorded at the sampling rate of 2 Hz. A digital image correlation (DIC) system (VIC-2D) was also used to capture deformations of the half beams and thus detect cracks of the front concrete surface. In order to facilitate the digital image correlation measurements, adequate contrast in the gray scale of individual objects was required. This was achieved by using black and white spray paint to apply a stochastic speckle pattern.

4 Experimental Results

4.1 Material Properties

The measured material properties, determined after a curing period, are given in Table 2, and the associated failure
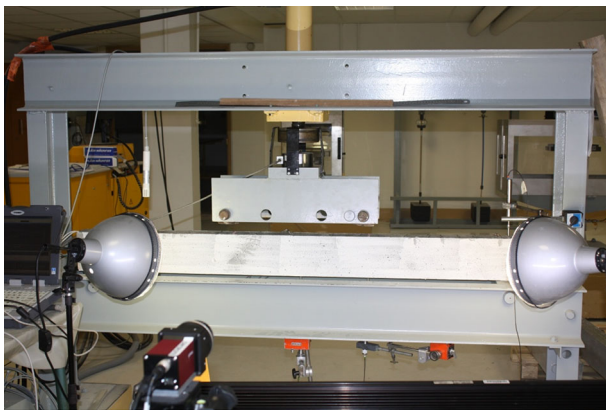

Fig. 3 Test setup and instrumentation

modes are shown in Fig. 6. Mean values and the associated standard deviations are also given. It can be seen from the results that for the adopted concrete formulation, fibers with a volume fraction $V_f = 1.27\%$ do not enhance the compressive strength (87 MPa instead of 85 MPa). The results from [31] underlined that up to the fibers' volume fraction of 0.5% mechanical characteristics of SFRC remain similar to plain concrete. On the contrary, regarding the splitting tensile strength measured, it can be seen that steel fibers improve significantly its value. The average increment of the splitting tensile strength of SFRC was 228% compared to the ordinary concrete. A similar observation was found by [32]. Similarly, to the splitting tensile strength, the flexural tensile strength also increased considerably (about 145%) with the addition of steel fibers. The mechanism for the increase in the flexural tensile strength is attributed to the strong fiber–matrix bond. Fibers inhibit formation and propagation of tensile cracks in concrete; this explains the higher tensile strengths obtained. Similar observations were also reported by [33]. The flexural tensile stress and deflection curves of ordinary concrete and SFRC beams are shown in Fig. 5. The flexural tensile stress F_{cf} is calculated by:

$$F_{cf} = \frac{P \times l}{d_1 \times d_2^2}$$

where P is the applied vertical load, d_1, d_2 and l are the width, depth and span length of the beam, respectively. The deflection is measured by an LVDT located at the midspan. It can be seen from Fig. 5 that for ordinary concrete beams without fibers, the failure occurs in a brittle way. This is marked by a sudden drop in the flexural load once the initial crack is formed in concrete. The stress/deflexion curve is linear up to the initial crack which is around 4.5 MPa. On the other hand, for steel fiber-reinforced concrete beams, the behavior is also linear elastic up to the initial crack, which this time is around 6.0 MPa. The incorporation of steel fibers to concrete has a positive effect on the first crack strength (a gain of 33%). After the post-elastic phase, and contrary to the unreinforced beams, the SFRC beams showed a deflection-hardening behavior up to the ultimate strength, which represents approximately two times the first cracking strength, revealing a higher load-carrying aptitude after the initial cracking. Furthermore, after the post-peak phase, a very large ductility was observed. The displacement increases with a smooth drop of the applied stress. The post-elastic and post-peak phases denote the beneficial effect of steel fibers on retarding the propagation of the cracks and enhancing the tensile and ductility performance of the concrete. The effect of hardening behavior was also observed in [14, 34] studies for SFRC beams with fiber volume fractions of 0.75% and 1% (Fig. 6).
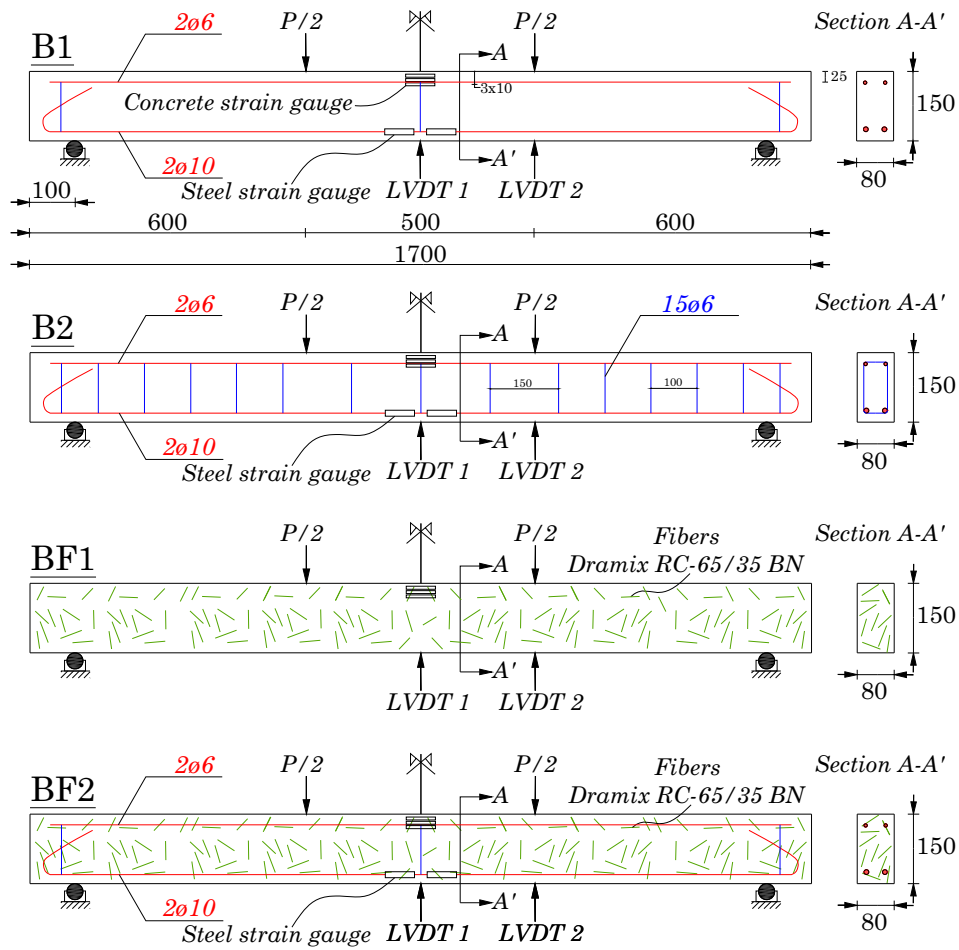
Fig. 4 Geometry, reinforcement details of beams and transducers' position

Table 2 Summary of material properties

Name of the beams	Compressive strength (MPa)		Splitting tensile strength (MPa)		Flexural tensile strength (MPa)		Young modulus (GPa)	
	Mean	Standard deviation	Mean	Standard deviation	Mean	Standard deviation	Mean	Standard deviation
B1	85	1.00	2.70	0.32	4.50	0.30	33.90	0.71
B2	85	1.00	2.70	0.32	4.50	0.30	33.90	0.71
BF1	87	2.08	8.86	0.77	11.03	2.30	35.30	0.92
BF2	87	2.08	8.86	0.77	11.03	2.30	35.30	0.92
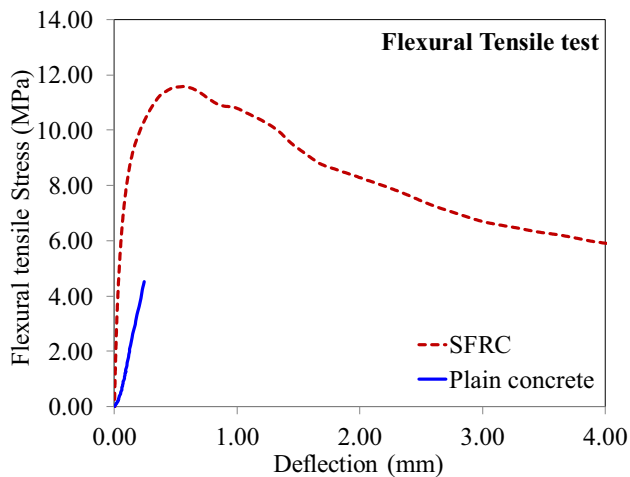
Fig. 5 Flexural tensile stress–deflection curves of the prismatic beam specimens

4.2 Comparisons Between Non-fiber-Reinforced Beams

4.2.1 Global and Local Behaviors

The ultimate loads obtained are summarized in Table 3. Figure 7a shows the load/deflection curves of the non-fiber-reinforced beams B1 and B2. For the first beam B1 without shear reinforcement, the failure occurs in a very brittle manner, with a drop of the bearing capacity once shear cracks appear for a loading level of 20 kN. Such a failure type is highly undesirable. On the other hand, beam B2 with adequate shear reinforcement showed a great increase in the bearing capacity and displacement at failure. The gain is 158% (58.37 kN against 22.65 kN) for displacements up to 38 mm against only 9 mm for the beam B1. The load/displacement curve of beam B2 is quasi-similar to the first beam B1 up to a loading level of 20 kN and keeps the same stiffness up to 42 kN. Then comes a plastic phase during which the load increases very slowly with the increase in the displacement until the failure, reflecting a ductile behavior. On the beam B2 curve, there is a very slight change of slope at a load level 16.5 kN (Fig. 7b) associated with a slight decrease in stiffness, which corresponds to the appearance of the shear crack (confirmed by digital image correlation, see Fig. 13) immediately taken over by the stirrups. It is clear that transverse reinforcement plays a key role in the bearing of shear load. Following the primary objective of this study, we will now seek to know how the fibers can play this role in the case where they substitute the transverse reinforcement.

To determine the yield points of beams B1 and B2, the applied load versus bottom longitudinal bars strain curves are plotted in Fig. 8a. For beam B1, without stirrups, the

failure occurs suddenly, and the maximum deformation (does not exceed 0.25%) remains in the elastic domain. This confirms that the failure intervenes by shear and not by bending. On the other hand, for B2, the longitudinal bars undergo plastic deformations from 0.25 up to 2.28% and play their full part in the flexural resistance of the beam. The flexural load versus strain curves measured on the concrete are shown in Fig. 8b and c and give an idea of the evolution of cracking on the surface of the beam. For all the strain gauges of beam B1, the deformation increases linearly after the effective loading of the beam to about 3 kN. The beam behaves in compression at the gauges in the top and middle positions, while it behaves in tension at the gauge in the low position. The load versus strain curve of beam B2 is linear up to a load level of 45 kN. Beyond this load, comes the concrete plastic phase. The deformation remains almost zero for the gauge at the middle position which means that this gauge is at the level of the neutral axis. Beyond 50 kN loading level, for the gauge at the low position, the concrete shows a perfectly plastic behavior since the deformation increases while the load remains constant.
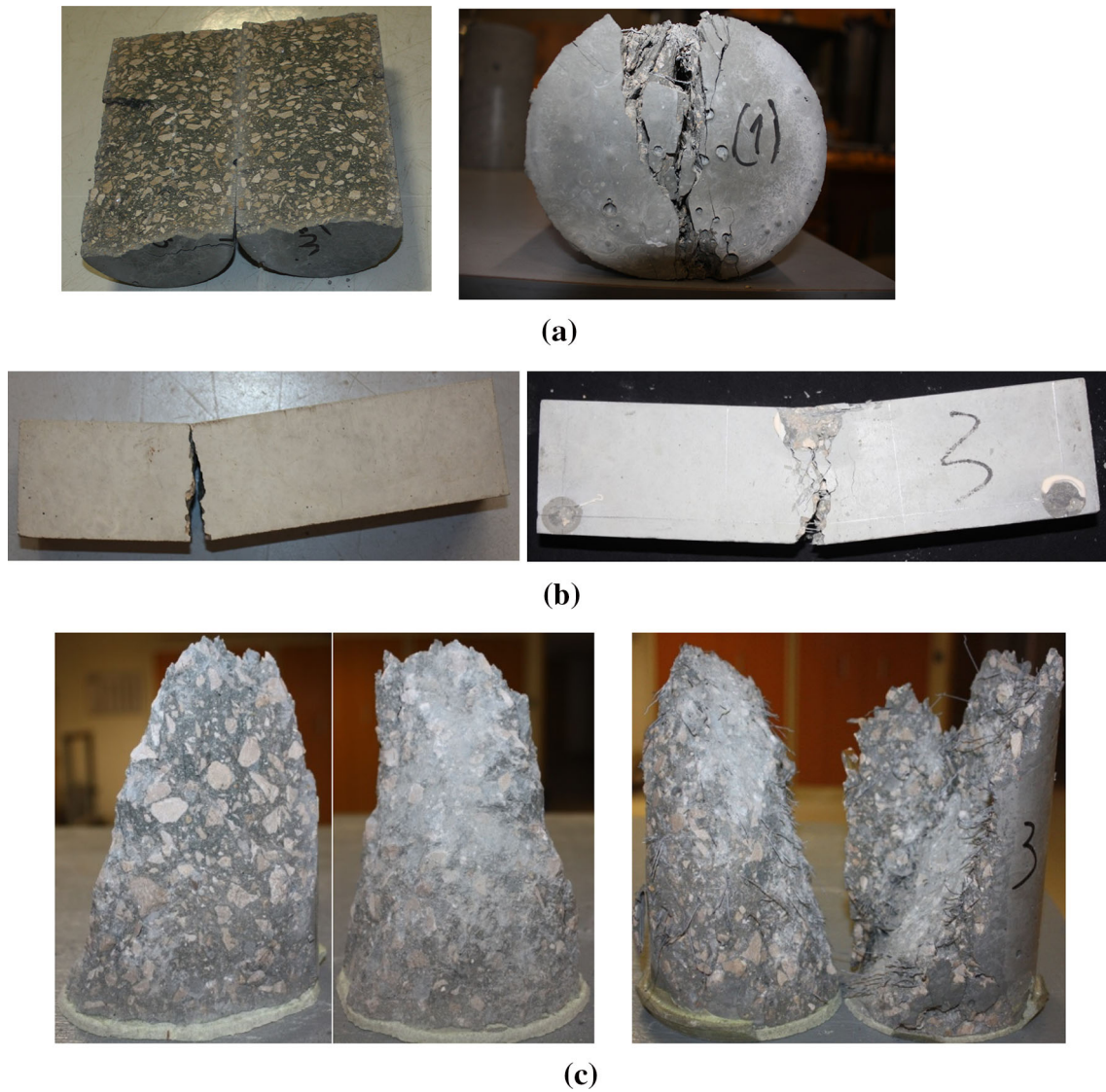
4.2.2 Failure Modes

The cracking patterns of the non-fiber-reinforced beams B1 and B2 are presented in Fig. 9. As it can be seen, and as expected, beam B1 failed in shear mode due to the absence of transverse reinforcement. The failure occurred quickly after the appearance of critical shear cracks located near the supports of the beam. Note that there are only three cracks associated with the great crack spacing on the entire beam. Beam B2 with stirrups failed in a flexural failure mode. The number of flexural cracks clearly increased with a decrease in the spacing between them, indicating a better distribution of loads.

4.3 Steel Fibers Versus Traditional Transverse Reinforcement Effect

4.3.1 Global and Local Behavior

The comparisons between the steel fibers and traditional transverse reinforcement, in order to investigate whether the use of steel fibers allows eliminating the traditional transverse reinforcement, are shown in Fig. 10. Beams B2 and BF2 test results were used for this examination. As a reminder, the beam B2 has a bottom longitudinal reinforcement ratio of $\rho = 1.30\%$ and adequate transverse reinforcement consisting of vertical stirrups with a diameter of 6 mm, spaced 150 mm apart at maximum, and BF2 has the same longitudinal reinforcement ratio and a fiber volume fraction of 1.27% (100 kg/m^3). The load–

Fig. 6 Failure modes and crack pattern of plain and fiber-reinforced concrete: **a** splitting tensile test; **b** flexural tensile test; **b** uniaxial compressive test

Table 3 Summary of experimental results

Name of the beams	Initial cracking load (kN)	Ultimate load (kN)	Displacement at ultimate load (mm)	Failure mode
B1	3.10	22.65	8.94	Shear
B2	3.12	58.37	38.05	Bending
BF1	6.85	9.18	30.69	Bending
BF2	4.60	58.77	40.01	Bending

deflection curves of beams B2 and BF2 given in Fig. 10 showed obviously that fibers with a volume fraction of 1.27% can completely replace the transverse reinforcement. The two curves are very similar to an elastic and a large plastic phase. The maximum deflection reaches almost 40 mm in both cases for an identical flexural

resistance of 58 kN, which reflects also for beam BF2 a ductile behavior. Figure 10b shows an emphasis on the appearance of initial cracks marked by the first slope change in the load–deflection curves. The first crack appearance corresponds to a load of 3.12 kN for non-fiber-reinforced beam B2, versus 4.6 kN for beam BF2 with
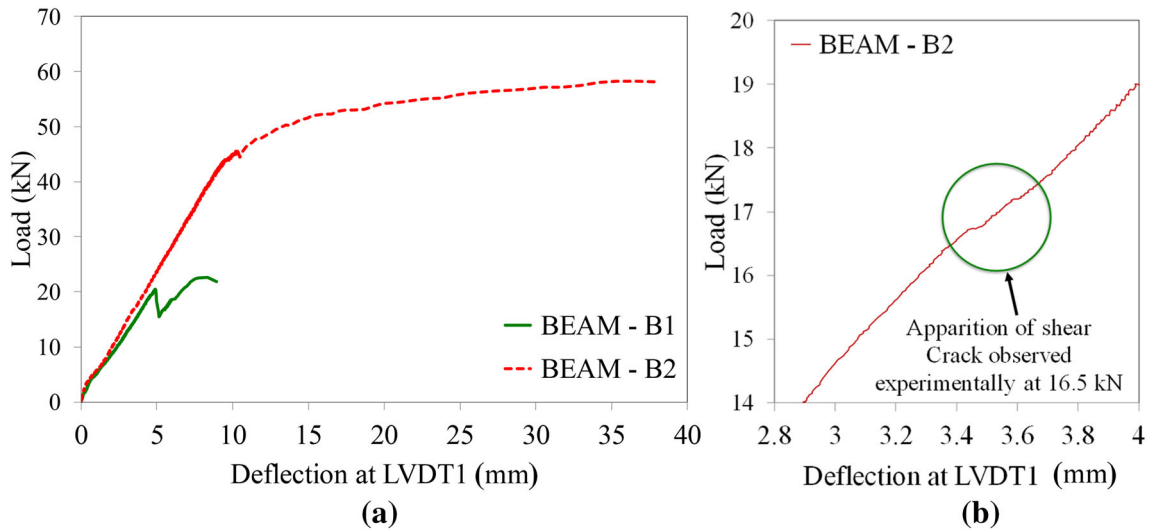
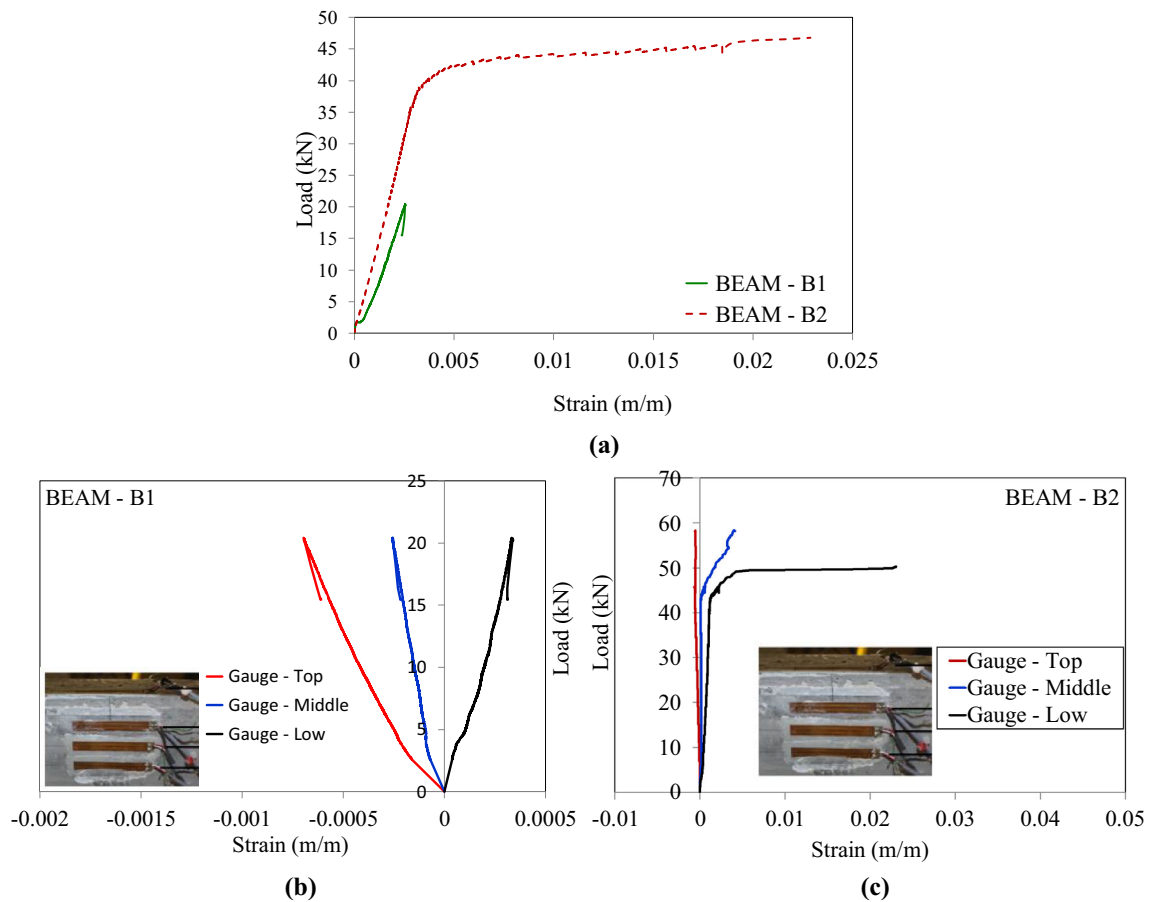Fig. 7 a Load–deflection curves of non-fiber-reinforced beams; b shear crack apparition for beam B2

Fig. 8 a Flexural load versus strain measured at longitudinal bars for B1 and B2; flexural load versus strain measured on concrete: b for B1, c for B2

fibers. Similarly, and confirmed by the digital image correlation (Fig. 13), shear crack initiation occurs much earlier for non-fiber-reinforced beam (16.5 kN vs. 45 kN).

This behavior can be attributed to fibers. The fibers and their dispersion within the cementitious matrix allow inhibiting the initiation and growth of cracks at the micro-
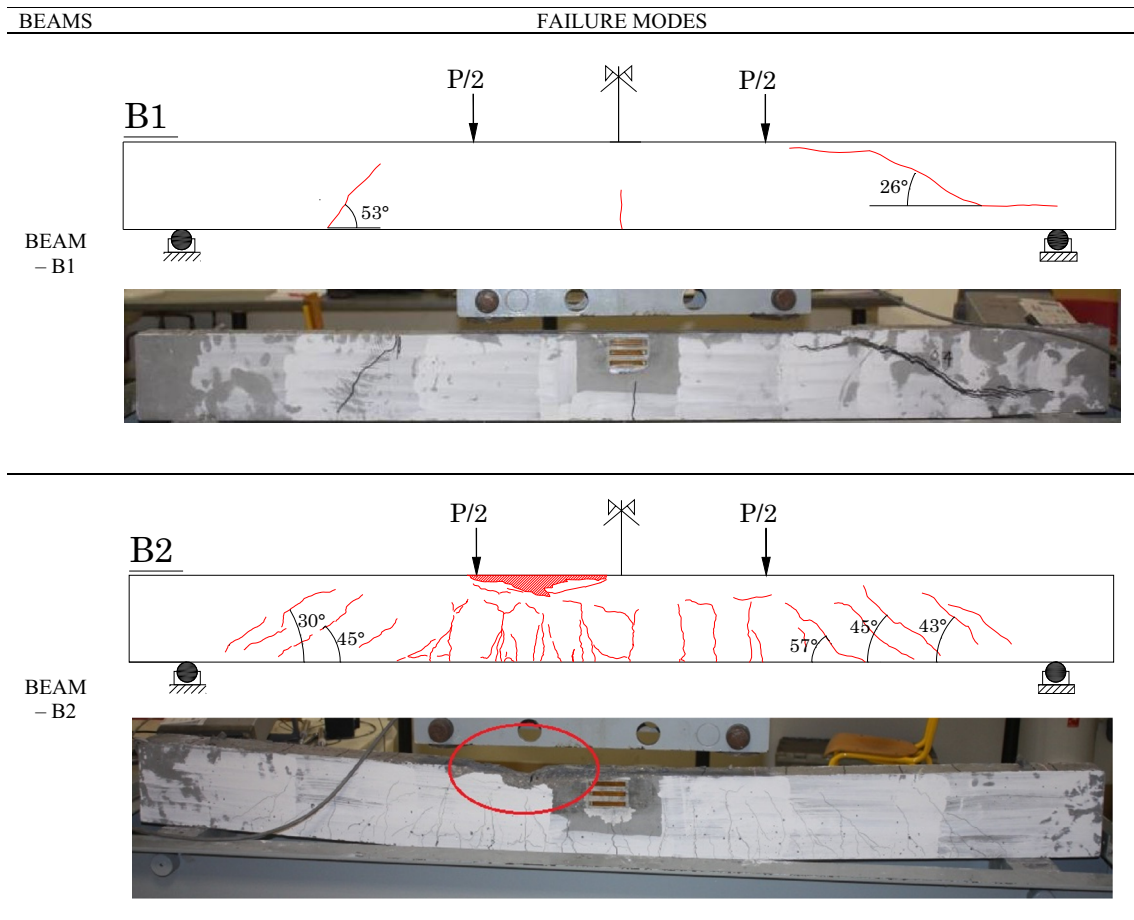
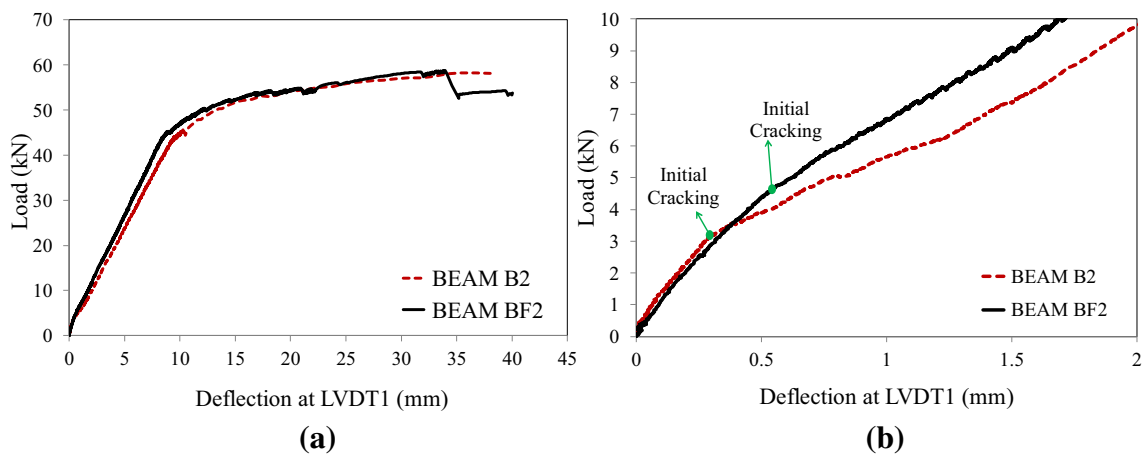**Fig. 9** Crack pattern of non-fiber-reinforced beams B1 and B2

Fig. 10 Steel fibers versus traditional transverse reinforcement effect: **a** load–deflection curves; **b** initial cracking

level before they are visible; then, they can provide effective bridging at the macro-level. This is valid for both

vertical flexural cracks and inclined shear cracks since fibers are randomly distributed in all positions. It can also

be seen that the post-elastic stiffness is slightly higher in the case of steel fiber-reinforced beam BF2. The effect of steel fibers on the post-elastic flexural stiffness is more noticeable when observing the load–deflection curves of beams B1 and BF2 (Fig. 11). As a reminder, beam B1 has an identical steel bar reinforcement arrangement as BF2 but without steel fiber reinforcement. It appears that the steel fibers improve the post-elastic stiffness, and this is due to their capability to hamper the crack propagation to the compressive zone by resisting tensile stresses at the crack surface. Similar observations were reported in [14, 34] studies.

The load versus rebar strain curves of beams B2 and BF2 are plotted in Fig. 12a. As noticed for load–deflection curves, the two load–strain curves are also very similar. Similarly, to beam B2 where the longitudinal rebars exhibit plastic deformations from 0.25 up to 2.28%, the longitudinal rebars of beam BF2 also undergo plastic deformations up to 3.15%. We recall that it is not the case for beam B1 which has no steel fibers and no shear reinforcement. This proves once again that the high volume of metallic fibers here used ($V_f = 1.27\%$) permits to perfectly replace the shear reinforcement. The load versus concrete strain curves for beam BF2 are shown in Fig. 12b. As for beam B2, the curve progresses linearly up to a load level of 45 kN, which also precedes a phase of plastic behavior of concrete. Beyond 50 kN and 58 kN loading levels, for the gauges at the low and middle positions, respectively, the concrete shows perfectly plastic behaviors.

4.3.2 Failure Modes

The observed cracking pattern of beam BF2 is presented in Fig. 14. The evolution of cracking throughout loading is also provided by the digital image correlation both for beam B2 and BF2 (Fig. 13). The cracking pattern of SFRC beam BF2 is very similar to that of the beam B2 (Fig. 9).
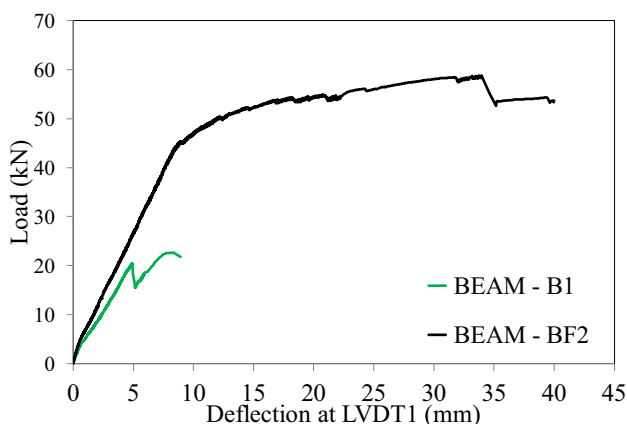
Fig. 11 Load–deflection curves of beams B1 and BF2

The evolution of the cracks is also the same in both cases but is slightly out of step since they appear later in the case of SFRC. In both cases, the failure occurs in bending. Note also that there is a main flexural crack for BF2, while there are several cracks of equivalent size for the non-fiber-reinforced beam B2. Figure 13 shows the apparitions of initial cracks (3.12 kN vs. 4.6 kN) and shear cracks (16.5 kN vs. 45 kN) for beams B2 and BF2 (Fig. 14).

4.4 Examination of the Effect of a Combination of Fibers and Longitudinal Reinforcement

4.4.1 Global and Local Behaviors

Figure 15 shows the effect of longitudinal reinforcement on the flexural behavior of SFRC beams. The test results for the entirely SFRC beam BF1 and beam BF2 combining longitudinal and steel fiber reinforcements were used for the investigation. The load–deflection curves of the considered beams are very different. For beam BF1, the ultimate flexural capacity does not exceed 10 kN while it reaches almost 60 kN, i.e., six times more with longitudinal reinforcement. This corresponds to a considerable resistance gain of 500% for a bottom longitudinal reinforcement ratio passing from $\rho = 0\%$ to $\rho = 1.30\%$. The beam BF1 exhibits a linear elastic behavior up to a loading level of 7 kN at which the initial crack appeared. Up to this loading level, the same slope for both beams BF1 and BF2 is obtained. Then, the beam BF1 quickly exhibits a ductile behavior as the load decreases very gradually until the failure occurs for a 30-mm mid-span deflection. As discussed before and now compared to beam BF1, beam BF2 presents an earlier first crack apparition at a loading level of 4.6 kN, followed by a linear part up to the appearance of shear crack initiation at 45 kN. Then comes a plastic phase with a much lower slope due to flexural stiffness reduction up to 58 kN for a 40-mm mid-span deflection. The flexural load versus strain curves measured on the concrete for beam BF1 are shown in Fig. 15b. The deformation values remain low and less than 0.001 m/m. Nevertheless, it is observed that the deformations increase linearly with the load in the legible part of the curve. The deformation of the beam does not reach the stage of plastic behavior of the concrete, the failure occurs before.

4.4.2 Failure Modes

The observed cracking pattern of beam BF1 is presented in Fig. 16. As regards cracking, the behavior of BF1 and BF2 (Fig. 14) is again very different. The beam BF1 has only four cracks, all included between the two loading points. There is a very important crack almost in the center of the beam, through which the failure occurs by sliding and
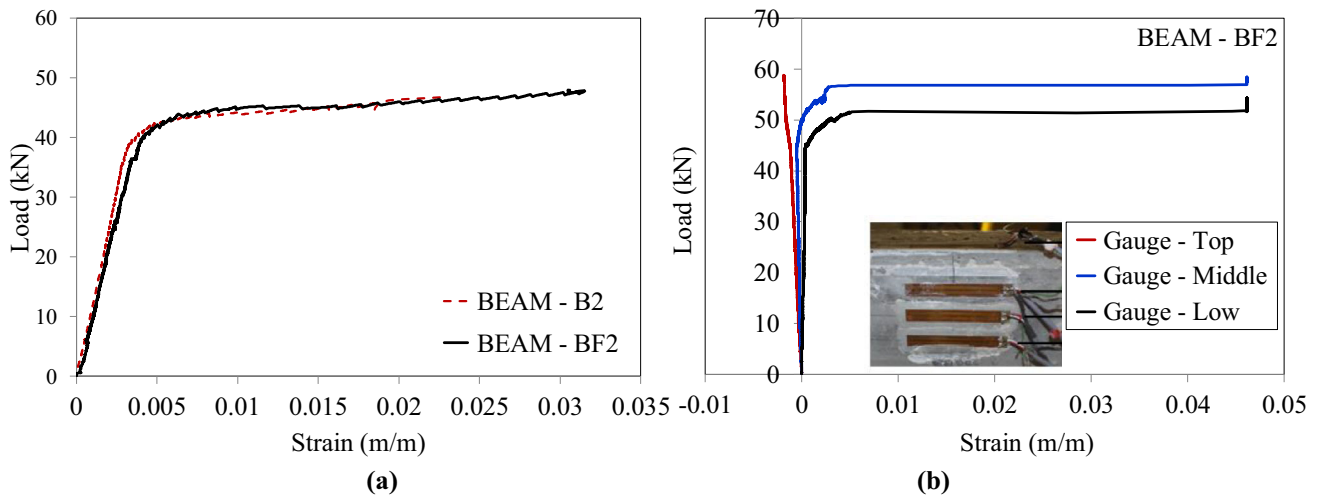
Fig. 12 **a** Flexural load versus strain measured at longitudinal bars for BF2 and B2; **b** flexural load versus strain measured on concrete

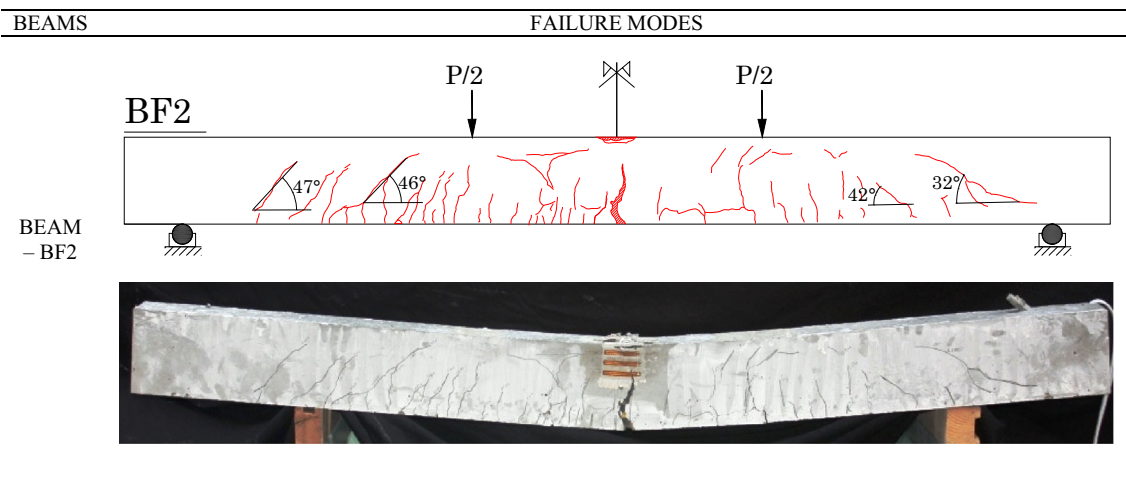**Fig. 13** Cracking propagation of beams B2 and BF2 captured by digital image correlation

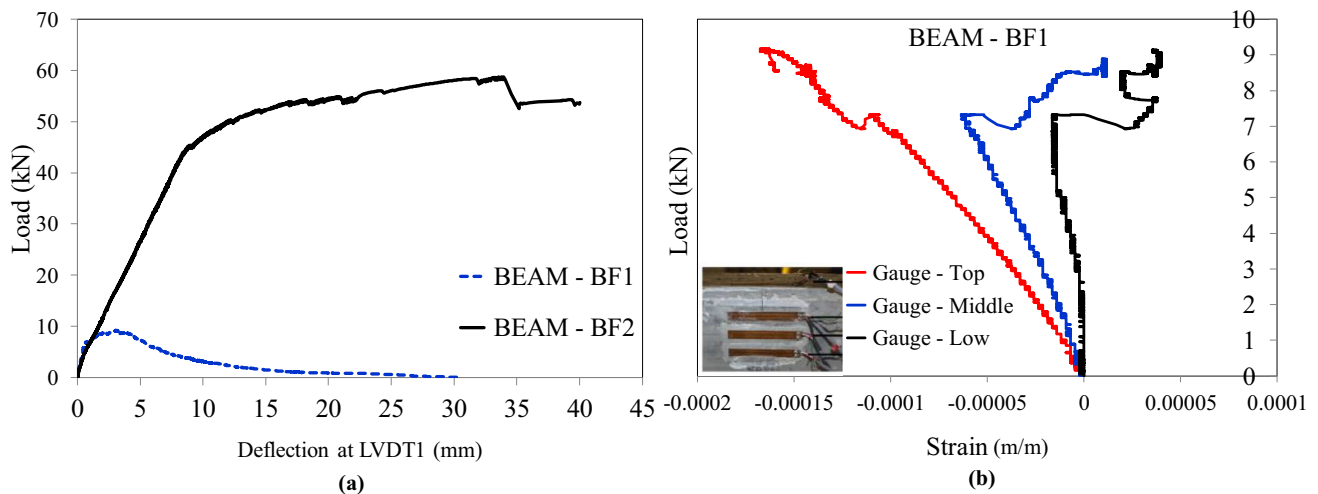**Fig. 14** Failure mode and crack pattern of beam BF2

Fig. 15 Steel fibers and longitudinal reinforcement combination effect: **a** Load–deflection curves of BF1 and BF2; **b** flexural load versus strain measured on concrete

breaking of the fibers. The failure occurs by bending. The fibers seem to carry shear loads since no inclined cracks have been observed. The beam BF2 as discussed previously shows many more cracks, distributed between the two supports homogeneously. We also note the presence of a significant crack in the center of the beam, which involves bending failure. The distribution of the loads is much better given the location of the cracks which reflects a good implication of the longitudinal bars.

Ultimately, although fibers are effective in bearing shear loads and provide a ductile material, they are not enough by themselves to ensure adequate resistance under bending failure. To achieve this, it is necessary to add longitudinal reinforcements which allow carrying large-sized flexural cracks. In this case, one can obtain behavior quite similar to conventional reinforced concrete with shear reinforcement. Longitudinal reinforcement bars play a significant role with regard to cracking. In their absence, even with fibers, cracks are few but their opening is quickly very important. The cracks' opening cannot be obstructed by fibers which slide through the cement matrix. The presence of bottom longitudinal reinforcement allows, in addition to the homogeneous distribution of numerous cracks along the beam, to limit their opening. The cracks' opening is also important at failure, but it occurs much later, at higher loads and deflections. Longitudinal reinforcements are therefore essential to ensure good control of the cracks' opening.
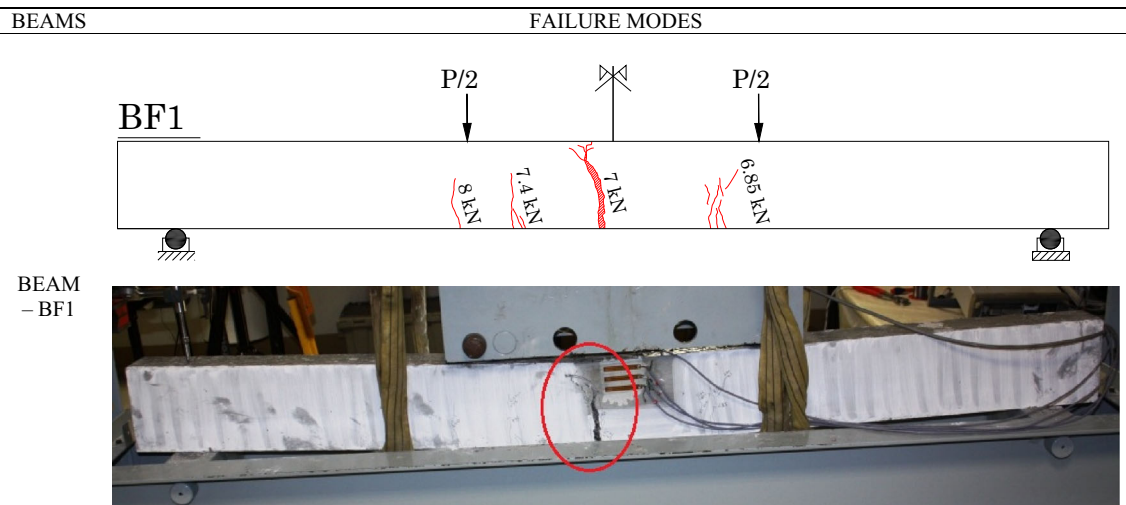
BEAMS   FAILURE MODES

Fig. 16 Failure mode and crack pattern of beam BF1

5 Conclusions

This exploratory study investigates the effect of steel fibers on bending and shear behavior of RC beams with high-strength concrete. The main objective was to examine the possibility of replacing stirrups, or traditional transverse reinforcement, by steel fibers and to study the effect on the beam structural behavior when steel fibers are combined with longitudinal reinforcement. For this purpose, an experimental program including four beam specimens with different configurations was considered. Ahead of the beams' strength tests, preliminary characterization tests of the non-reinforced concrete and the steel fiber-reinforced concrete were carried out. The following conclusions were drawn:

- The material tests of SFRC showed that the concrete compressive strength was weakly sensitive to the incorporation of steel fiber. A compressive strength gain of only 2% was obtained by increasing the fiber quantity from 0 kg to 100 kg/m^3 which is equivalent to a volume fraction from zero to 1.27%. However, in regard to the splitting tensile strength and flexural tensile strength, the addition of steel fibers improves significantly their values, up to 228% and 145%, respectively. Contrary to ordinary concrete, the SFRC showed after the elastic phase, a hardening behavior up to the ultimate strength, and the post-peak phase was characterized by a very large ductility. These reflect a higher load-carrying capacity after initial cracking, steel fibers allow delaying cracks propagation and opening, and thus enhance the tensile and ductility performance of the concrete.

- In the particular case here studied, a high volume of metallic fibers ($V_f > 1.2\%$) allows to obtain a substantial shear capacity and ductile collapse of the beam.

- Fibers with a high-volume fraction of 1.27% (100 kg/m^3) are able to completely replace the traditional transverse reinforcement (stirrups) both in terms of flexural resistance and failure mode. Initial cracking appeared early for non-fiber-reinforced beam compared to the counterpart beam with fiber, due to the fiber aptitude to bridge the cracks at the micro-cracking stage. This has been confirmed by digital image correlation analysis. It was also found that the steel fibers improve the structural post-elastic stiffness, and this is due to their capability to hamper the crack propagation to the compressive zone by resisting to tensile stresses at the crack surface.

- Although fibers with a volume fraction of 1.27% (100 kg/m^3) are effective in bearing shear loads and provide a ductile behavior, they are not enough by themselves to ensure an optimum resistance due to the presence of bending load. To achieve this, it is necessary to add longitudinal reinforcements which allow carrying large-sized flexural cracks, but also a good distribution of the internal loads. In this case, one can obtain a behavior at least similar to conventional reinforced concrete beam structure with longitudinal and shear reinforcement.

In most practical applications of SFRC modular construction, with classical shear reinforcement ratios adopted for beams' design, it is possible to completely replace the traditional transverse reinforcement or stirrups by fibers on the condition of using a sufficient fiber volume fraction. Considering metallic fibers proportion, 100 kg/m^3 is not a

common ratio. Replacement of shear steel reinforcements in any configuration has to be studied in detail for different configurations and needs more extensive research. A complementary study has to be conducted also for high shear reinforcement ratios.

Compliance with Ethical Standards

Conflict of Interest On behalf of all authors, the corresponding author states that there is no conflict of interest.

References

1. Li J, Wu C, Liu Z-X (2018) Comparative evaluation of steel wire mesh, steel fibre and high performance polyethylene fibre reinforced concrete slabs in blast tests. Thin Walled Struct 126:117–126. https://doi.org/10.1016/j.tws.2017.05.023
2. Lee J-H, Cho B, Choi E (2017) Flexural capacity of fiber reinforced concrete with a consideration of concrete strength and fiber content. Constr Build Mater 138:222–231. https://doi.org/10.1016/j.conbuildmat.2017.01.096
3. Jen G, Trono W, Ostertag CP (2016) Self-consolidating hybrid fiber reinforced concrete: development, properties and composite behavior. Constr Build Mater 104:63–71. https://doi.org/10.1016/j.conbuildmat.2015.12.062
4. Lee J-H, Cho B, Choi E, Kim Y-H (2016) Experimental study of the reinforcement effect of macro-type high strength polypropylene on the flexural capacity of concrete. Constr Build Mater 126:967–975. https://doi.org/10.1016/j.conbuildmat.2016.09.017
5. Kwak Y-K, Eberhard MO, Kim W-S, Kim J (2002) Shear strength of steel fiber-reinforced concrete beams without stirrups. ACI Struct J 99:530–538. https://doi.org/10.14359/12122
6. Amin A, Foster SJ (2016) Shear strength of steel fibre reinforced concrete beams with stirrups. Eng Struct 111:323–332. https://doi.org/10.1016/j.engstruct.2015.12.026
7. Khuntia M, Stojadinovic B, Goel SC (1999) Shear strength of normal and high-strength fiber reinforced concrete beams without stirrups. Struct J 96:282–289. https://doi.org/10.14359/620
8. Yermak N, Pliya P, Beaucour A-L, Simon A, Noumowé A (2017) Influence of steel and/or polypropylene fibres on the behaviour of concrete at high temperature: spalling, transfer and mechanical properties. Constr Build Mater 132:240–250. https://doi.org/10.1016/j.conbuildmat.2016.11.120
9. Doan QH, Lee DK, Lee JH, Kang JW (2019) Design of buckling constrained multiphase material structures using continuum topology optimization. Meccanica 54:1179–1201. https://doi.org/10.1007/s11012-019-01009-z
10. Nguyen AP, Banh TT, Lee DK, Lee JH, Kang JW, Shin SM (2018) Design of multiphase carbon fiber reinforcement of crack existing concrete structures using topology optimization. Steel Compos Struct 29(5):635–645
11. Yoo D-Y, Banthia N (2017) Mechanical and structural behaviors of ultra-high-performance fiber-reinforced concrete subjected to impact and blast. Constr Build Mater 149:416–431. https://doi.org/10.1016/j.conbuildmat.2017.05.136
12. Chalioris CE (2013) Steel fibrous RC beams subjected to cyclic deformations under predominant shear. Eng Struct 49:104–118. https://doi.org/10.1016/j.engstruct.2012.10.010
13. Winkler A, Edvardsen C, Kasper T (2017) Examples of bridge, tunnel lining and foundation design with steel-fibre-reinforced concrete. SP 310:451–460
14. Yoo D-Y, Moon D-Y (2018) Effect of steel fibers on the flexural behavior of RC beams with very low reinforcement ratios. Constr Build Mater 188:237–254. https://doi.org/10.1016/j.conbuildmat.2018.08.099
15. Wille K, El-Tawil S, Naaman AE (2014) Properties of strain hardening ultra high performance fiber reinforced concrete (UHP-FRC) under direct tensile loading. Cement Concr Compos 48:53–66. https://doi.org/10.1016/j.cemconcomp.2013.12.015
16. di Prisco M, Colombo M, Dozio D (2013) Fibre-reinforced concrete in fib Model Code 2010: principles, models and test validation. Struct Concr 14:342–361. https://doi.org/10.1002/suco.201300021
17. Gharehbaghi K, Chenery R (2017) Fiber reinforced concrete (FRC) for high rise construction: case studies. IOP Conf Ser Mater Sci Eng 272:012034. https://doi.org/10.1088/1757-899X/272/1/012034
18. Dancygier AN, Savir Z (2006) Flexural behavior of HSFRC with low reinforcement ratios. Eng Struct 28:1503–1512. https://doi.org/10.1016/j.engstruct.2006.02.005
19. Vandewalle L, Nemegeer D, Balazs L et al (2001) RILEM TC162-TDF: test and design methods for steel fibre reinforced concrete: uni-axial tension test. Mater Struct 34:3–6
20. Paegle I. Evaluation of test methods used to characterize fiber reinforced cementitious composites. In: Proceedings of the international conference "Innovative materials, structures and technologies"; 2013. p. 122–8.
21. fib (2010) fib model code for concrete structures. Wiley, New York. https://doi.org/10.1002/9783433604090
22. SS 812310:2014. Fibre concrete—design of fibre concrete structures. Swedish Standards Institute, Stockholm; 2014. p. 1–38.
23. CEN. EN 14651: test method for metallic fibered concrete: measuring the flexural tensile strength (limit of proportionality (LOP), residual). European committee for standardization, Bruselas; 2005.
24. RILEM TC 162-TDF. Recommendations of RILEM TC 162-TDF: test and design methods for steel fibre reinforced concrete: bending test. Mater. Struct. 2002;35:579–82. https://doi.org/10.1617/13884.
25. Japan Concrete Institute Standard (2006) Method of test for bending moment-curvature curve of fiber-reinforced cementitious composites. J Adv Concr Technol 4:73–78. https://doi.org/10.3151/jact.4.73
26. Paegle I. Characterization and modeling of fiber reinforced concrete for structural applications in beams and plates, vol. 327. Byg Rapport. Technical University of Denmark, Department of Civil Engineering; 2015.
27. EN 12390-5. Testing hardened concrete—part 5: flexural strength. AFNOR; 2012.
28. CEN. Eurocode 2. Design of concrete structures—part 1-1: general rules and rules for buildings. EN 1992-1-1. Bruss Com Eur Norm CEN 2005. n.d.
29. Dinh HH, Parra-Montesinos GJ, Wight JK (2010) Shear behavior of steel fiber-reinforced concrete beams without stirrup reinforcement. Struct J 107:597–606. https://doi.org/10.14359/51663913
30. Minelli F, Plizzari GA (2013) On the effectiveness of steel fibers as shear reinforcement. Struct J 110:379–390. https://doi.org/10.14359/51685596

31. Yazıcı Ş, İnan G, Tabak V (2007) Effect of aspect ratio and volume fraction of steel fiber on the mechanical properties of SFRC. Constr Build Mater 21:1250–1253. https://doi.org/10.1016/j.conbuildmat.2006.05.025

32. Gao J, Sun W, Morino K (1997) Mechanical properties of steel fiber-reinforced, high-strength, lightweight concrete. Cement Concr Compos 19:307–313. https://doi.org/10.1016/S0958-9465(97)00023-1

33. Yoo D-Y, Yoon Y-S, Banthia N (2015) Predicting the post-cracking behavior of normal- and high-strength steel-fiber-reinforced concrete beams. Constr Build Mater 93:477–485. https://doi.org/10.1016/j.conbuildmat.2015.06.006

34. Altun F, Haktanir T, Ari K (2007) Effects of steel fiber addition on mechanical properties of concrete and RC beams. Constr Build Mater 21:654–661. https://doi.org/10.1016/j.conbuildmat.2005.12.006